SSRG International Journal of Electrical and Electronics Engineering
ISSN: 2348-8379/ https://doi.org/10.14445/23488379/IJEEE-V11I3P122

Volume 11 Issue 3, 269-279, March 2024

Original Article

Performance of Amplitude Probabilistic Shaping Based on Modified Multi-Repeat Mapping in Wireless Fading Channels

Ali Shaban Hassooni[1,2]*, Laith Ali Abdul Rahaim[1]

[1]*Department of Electrical Engineering, College of Engineering, University of Babylon in Hilla, Iraq.*
[2]*Department of Biomedical Engineering, College of Engineering, University of Babylon in Hilla, Iraq.*

**Corresponding Author : eng.ali.shaban@uobabylon.edu.iq*

Received: 15 January 2024 Revised: 11 February 2024 Accepted: 13 March 2024 Published: 25 March 2024

Abstract *- Probabilistic Amplitude Modulation (PAS) is one of the techniques that has attracted significant and increasing interest in recent years in improving system performance, bringing the data rate achievable to the Shannon limit, improving spectral efficiency, and reducing constellation power. This paper will analyse the average symbol error rate performance of Probability Amplitude Shaping (PAS). The discussion is based on a Modified Multi-Repeat Distribution Matcher (PAS-MMRDM) used for wireless communications in Gaussian and fading channels. The analysis includes four different fading models: Rayleigh channels, Log-normal fading channels, Nakagami-m channels, and Composite Log-Normal shadowing/Nakagami-m fading channels. Simulation supported and compared the results with input symbols for high-order modulation schemes such as uniform Quadrature Amplitude Modulation (QAM). It will also be noted that PAS based on MMRDM provides a significant improvement in the average symbol error rate at a certain Signal-to-Noise Ratio (SNR) or a significant decrease in the SNR wanted to perform specific symbol error probability compared to uniform QAM for different cases of channels, for example, the improvement in the net shaping gain of about 1.21, 1.64, and 1.81 dB at Symbol Error Rate (SER) with entropy rate 4, 6, and 8 bits/symbol, all cases at Symbol Error Ratio (SER)=* 10^{-4} *when compared with uniformly distributed symbols of QAM.*

Keywords *- Log-Normal shadowing, Nakagami-m fading, MMRDM, Probabilistic shaping, Rayleigh fading.*

1. Introduction

High Spectral Efficiency (SE) is one of the necessary and crucial requirements in future communication systems, where many techniques, such as channel coding, high-order modulation schemes, and others, play an essential role [1-3]. The traditional transmission of data in most communication systems cannot utilize channel capacity optimally [4] due to data having a uniform distribution that leads to a loss reaching 1.53 dB in achievable data rate (Shaping gap) [5]. Therefore, this transmission type is unsuitable for Additive-White-Gaussian Noise (AWGN) channels, and the performance will deteriorate significantly in the fading and multipath wireless channels [6].

Many studies have been conducted on a large scale regarding the probability of error in quadrature amplitude modulation, as well as pulse amplitude modulation in AWGN and fading channels [6-12]. In all these studies, the considered input symbols were the uniform distribution symbols. One of the crucial techniques that have gained increasing and pivotal interest in improving the quality of communication systems and overcoming (the shaping gap) is Probabilistic Shaping (PS) by optimizing the input symbols distribution through signal shaping to improve energy efficiency [4, 5].

The resulting distribution of the symbols is a Gaussian-like non-uniform distribution; by applying it to the QAM constellation, the transmitting probability of low-energy constellation points will increase (more repetition) while the transmitting probability of higher-energy points will decrease (less repetition). The commonly used distribution to generate non-uniform signalling is the Maxwell-Boltzmann (MB) distribution to close the shaping gap and maximize shaping gain to theoretically ($\pi e/6$ or 1.53 in dB) [5, 13].

PS is a technology based on trading off power efficiency for spectral efficiency. Many researchers [14-17] proposed various Probabilistic Shaping (PS) scenarios utilized in transmission systems, and the system performance has been improved in several respects. This reflects the importance of including probabilistic shaping as an essential part of various systems in communication structures.

Recently, there has been increasing interest in Probabilistic Amplitude Shaping (PAS) coded modulation as a method to integrate modulation schemes and channel coding. This approach has gained attention in various communication systems (wireless and optical).

The structure of PAS is based on a distribution matcher called the Constant Composition-Distribution-Matching (CCDM) algorithm, which uses arithmetic coding for shaping. The performance of CCDM improves with longer data packets, but this also increases the complexity of arithmetic coding [18]. Moreover, [19] provides further details on this topic.

Many researchers have developed a method to reduce short to medium-block length rate losses. They used Sphere Mapping to Distribution Matcher (SMDM) in [20]. In [14], a pas-based Enumerative Sphere Shaping (ESS) was proposed, which has been proven to perform better than CCDM for small or medium block lengths when evaluated via the AWGN channel.

The computational and storage complexity has also been reduced for short block lengths. However, ESS still has some limitations and computational complexity and required storage capacity becomes high, particularly with long data packets. In optical fiber communications and free space optical communications [4, 16, 21-25], the PS is presented as an optimum technique that achieves excellent transmission rates and distances and maximizes the transmission capacity and system performance.

This paper will provide an extended study of the symbol error performance of probabilistic shaping based on a modified distribution matcher called a Multi-Repeat Distribution Matcher (MRDM) [26] under AWGN and various fading channel types. This modification will create several small lookup tables or groups to generate a shaping scheme.

The storage capacity required will be significantly reduced in this process, and it does not need any complex calculations. The non-uniform distribution is a mechanism used to shape the probability distribution of symbols in digital communications.

This technique is similar to the well-known Maxwell-Boltzmann (MB) distribution. It can be achieved by selecting the optimum number of levels and symbols that will be repeated in each level. By doing so, small lookup tables can be generated, with the same levels required to form the shaping and deshaping coders.

The resulting distribution is then shaped according to the required shaping rate, which leads to the efficient use of available bandwidth and the reduction of the probability of errors. First, over the Gaussian noise channel, an analysis of the Symbol Error Rate (SER) for uncoded M-QAM using MMRDM is conducted, and a simple approach to analytical expressions of SER in terms of distribution parameters is introduced.

The performance of the proposed matcher will be compared with the traditional uniformly distributed M-QAM to give a more comprehensive picture of the results obtained. The PS-MMRDM approach will be extended to derive a simplified expression SER to estimate MMRDM performance under the influence of fading over Rayleigh, Log-normal, Nakagami-m, and composite channels (Log-normal shadowing/ Nakagami-m) under different conditions.

The relationship between the PAS-MMRDM and rate parameters is derived to optimize the Probability Mass Function (PMF), close it to MB distribution, and analyze its impact on system performance. By changing the number of levels (L) or repeating subsets mode, the rate parameter value can be controlled to provide the desired entropy.

The SNR gain is compared between uniform M-QAM and PAS-MMRDM for all channels in three entropy values according to 2 different levels (L); for example in AWGN channel, PS-MMRDM applied to 16-QAM, 64-QAM, and 256-QAM with levels (L) of MMRDM as L= {10,30} for 16-QAM, L={80,100} for 64-QAM, and L={300,360}for 256-QAM. The SNR enhancement gained about {4 , 2.2} dB for PAS-16-QAM, {4.86, 2.87} for PAS-64-QAM, and {5.1, 3.36} for PAS-256-QAM at SER = 10^{-4} compared with the same degree of conventional uniform QAM.

The theoretical results supported with MATLAB R2022b simulations show significant results for all channel cases. At the same time, a higher order non-uniform-MQAM is compared to uniform M-QAM, which are 16, 64, and 256 QAM at the same level of entropy (H), with values 4, 6, and 8 bit/symbol; similarly, PAS-M-QAM offers a gain in SNR about 1.21 dB, 1.64 dB, and 1.81 dB at SER = 10^{-4}.

The paper's remaining sections are organized as follows: The concept of MMRDM is described in section 2. Section 3 introduces the relations to generate non-uniform symbols in MMRDM. Section 4 of this study undertakes a comprehensive analysis of the symbol error performance of the modified distribution matcher across a range of channels.

Subsection 4.1. analyses the error performance over the AWGN channel is presented. Next, in subsection 4.2, the analysis is expanded to encompass additional fading channel conditions. Section 4.2.1 details the results under the Log-normal fading scenario. The Rayleigh fading channel is presented in subsection 4.2.2, and the Nakagami-m and Composite Log-Normal shadowing/Nakagami-m fading channels are presented in subsections 4.2.3 and 4.2.4. Section

5 provides an evaluation of the analytical and simulation results of the suggested distribution matcher for all channel types' conditions. The final section, Section 6, presents the conclusions.

2. Description of the Modified Distribution Matcher

In this work, MMRDM is used as Probabilistic shaping. This method is based on modified multiple repeat mapping of combinations rather than sequence permutation. Several lookup tables or sets are merged in this scheme to generate output sequences with the desired shaping rate, which translates to constellation points that resemble the MB distribution. The shaping process is illustrated in Figure 1 [26].

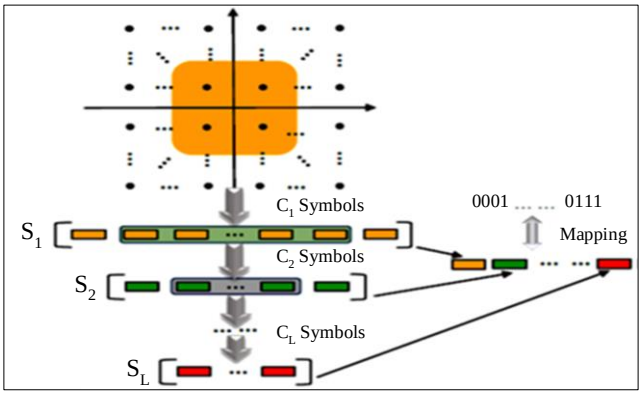

Fig. 1 Shaping process

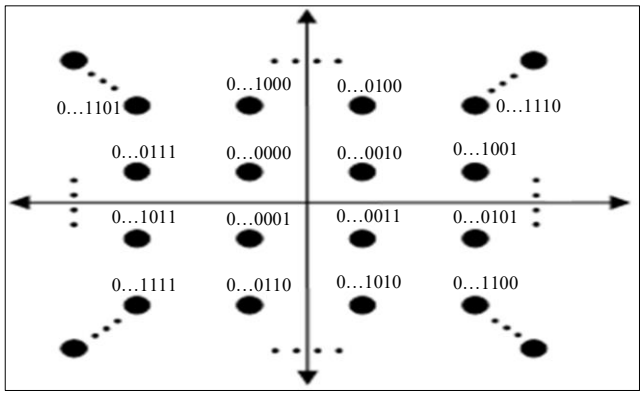

Fig. 2 Standard M-QAM constellation

As in [26], the term "L" represents the number of levels or groups, followed by the assignment of sub-groups, labelled as S_1, ..., S_L, each group consists of c_i symbols. Symbols are composed of a set of bits arranged in the same sequence as the constellation, representing the points of the constellation, as shown in Figure 2. A lookup table is generated for every level or subset. The tables provide a probabilistic representation of the input data for a certain packet length [26]. The energy rule governs symbol repetition; lower energy symbols repeat more often.

The shaping process achieved is based on several parameters that must be obtained: L levels, the N bits/symbol for M-constellation, $c_1, c_2, \ldots, c_L$ are the symbols repeated in each set group, and m is the packet length of the input data. Parameters are related to each other according to the following mathematical relationships [26]:

$$\begin{cases} c_1 \le 2^N \\ c_2 \le c_1 \\ \ldots\ \ldots \\ c_L \le c_{L-1} \\ 2^m \le c_1 \times c_2 \times \ldots \times c_L \le 2^{L \times N} \end{cases} \quad (1)$$

Suppose $\zeta_{PA'}$ is a set of vectors that satisfy the MB distribution PA', where

$$\zeta_{PA'} = c_1 \times c_2 \times \ldots \times c_L \quad (2)$$

Then the block length m will be:

$$m = \lfloor \log_2 c_1) \rfloor + \ldots + \lfloor \log_2 c_L) \rfloor \quad (3)$$

$\lfloor . \rfloor$ means taking an integer in the downward direction.

The rate (R) of shaping is,

$$R = {}^{m}/_{L \times N} \quad (4)$$

The size of the MRDM codebook is $|\mathrm{C}_{MRDM}| = 2^m$.

The parameter L determines how much the encoder can deviate from the MB distribution while maintaining a reasonable complexity. The maximum number of codewords that can be combined is $L \times 2^m$; each codeword contains L symbols, with each symbol containing N bits. To summarize, the MMRDM algorithm can be represented by the following pseudo-code.

Algorithm: MMRDM
Begin
{
Input: specified modulation order M

1. According to the modulation scheme, calculate N
2. Choose the number of levels L.
3. optimize the values of $c_1, c_2, \ldots, c_L$ based on the constraint Equation 1 and must follow Gaussian-like distribution with desired entropy.
4. Determine m according to the Equation 3
5. Calculate the rate R, according to Equation 4
6. Divide m to L groups; each group contain $\lfloor \log_2 c_i) \rfloor$ bits
7. Add extra bits for each group to construct N bits group

Output: L group, each group containing N bits mapped to symbols according to the M-QAM constellation in Figure 2.
{
End

M-QAM symbols probabilities are $p_A(a^M) = [p_{a1}, p_{a2}, \dots, p_{aM}]$, and there are L groups that have different probabilities; each group has ci symbols with probabilities as follows

Group g_1 consists of c_1 symbols with equal probabilities [26]:

$$p_{g_1}(a^{c1}) = [\frac{\frac{1}{c1}+\frac{1}{c2}+\dots+\frac{1}{cL}}{L}, \dots, \frac{\frac{1}{c1}+\frac{1}{c2}+\dots+\frac{1}{cL}}{L}]$$

Group g_2 consists of (c_2 - c_1) symbols with equal probabilities.

$$p_{g_2}(a^{c2}) = [\frac{\frac{1}{c2}+\dots+\frac{1}{cL}}{L}, \dots, \frac{\frac{1}{c2}+\dots+\frac{1}{cL}}{L}]$$

. . .

Group g_L consists of (c_L-c_{L-1}) symbols with equal probabilities.

$$p_{gL}(a^{cL}) = [\frac{\frac{1}{cL}}{L}, \dots, \frac{\frac{1}{cL}}{L}]$$

Then, the PS-QAM probabilities become

$$p_A(a^M) = p_{g_1} \cup p_{g_2} \cup \dots \cup p_{g_L}. \quad (5)$$

For example PAS-MMRDM 16-QAM, with L=3, c_1=4, c_2=8 c_3=16, m=9, the symbols probability will be,

$$p_A(a^{16}) = [\frac{\frac{1}{c1}+\frac{1}{c2}+\frac{1}{c3}}{L}, \frac{\frac{1}{c1}+\frac{1}{c2}+\frac{1}{c3}}{L}, \frac{\frac{1}{c1}+\frac{1}{c2}+\frac{1}{c3}}{L}, \frac{\frac{1}{c1}+\frac{1}{c2}+\frac{1}{c3}}{L}, \frac{\frac{1}{c1}+\frac{1}{c2}}{L}, \frac{\frac{1}{c1}+\frac{1}{c2}}{L}, \frac{\frac{1}{c1}+\frac{1}{c2}}{L}, \frac{\frac{1}{c1}+\frac{1}{c2}}{L}, \frac{\frac{1}{c2}}{L}, \frac{\frac{1}{c2}}{L}, \frac{\frac{1}{c2}}{L}, \frac{\frac{1}{c2}}{L}, \frac{\frac{1}{c2}}{L}, \frac{\frac{1}{c2}}{L}, \frac{\frac{1}{c2}}{L}, \frac{\frac{1}{c2}}{L}]$$

$$= [\frac{7}{48}, \frac{7}{48}, \frac{7}{48}, \frac{7}{48}, \frac{3}{48}, \frac{3}{48}, \frac{3}{48}, \frac{3}{48}, \frac{1}{48}, \frac{1}{48}, \frac{1}{48}, \frac{1}{48}, \frac{1}{48}, \frac{1}{48}, \frac{1}{48}, \frac{1}{48}] \quad (6)$$

Therefore, the storage capacity required in the proposed method is not $2^m \times (L \times N)$ bits as in [29] but will be [26]:

$$\text{Storage capacity} = (L \times log_2 M - m) \text{ bits} \quad (7)$$

If the selected subsets are the power of 2, but if any subset ***ci*** is not the power of 2, then the storage capacity of the lookup table for this subset will be

$$\text{Storage capacity} = (s_1 2^{s2} + s3) \quad (8)$$

Where,

$s_1 = s_2 = \lfloor log_2 ci \rfloor - 1$ and

$s_3 = log_2 M - (\lfloor log_2 ci \rfloor + 1)$.

As noted from Equations 7 and 8, the storage capacity required for the suggested method is extremely low, even for a higher order of modulation or for higher values of L when compared with [29], where the lookup table becomes impractical for high values of L, for example, in [29] L = N-1 for 64-QAM, the value of L = 5, if the rate R required is 2/3 the length of the output block n = 30 and the length of the input block m =20, thus becoming the necessary storage capacity to store the lookup table is $2^{20} \times 30$ bit, which is impractical, imagine for M 256 or 1024 QAM or larger value of L. In the proposed modification, the capacity required for the same parameters L, R, n, and m will be 10-bit according to Equation 7 [26].

3. PAS-MMRDM Symbols Generation

For M-QAM, $N = \log_2 M$ bits per symbol, and the constellation symbols' locations are *xi* = (±a, ±3a,…,±($\sqrt{M}-1$)a) + i(±a, ±3a,…,±($\sqrt{M}-1$)a). As mentioned before, the input symbols must be chosen from a commonly Maxwell-Boltzmann distribution to bring the channel capacity to the maximum in the Gaussian channel. The Maxwell-Boltzmann distribution can be represented as [5, 18],

$$p(x) = A(\lambda)e^{-\lambda|x|^2} \qquad x \in \mathrm{R} \quad (9)$$

The parameter $\lambda \geq 0$ plays a crucial role in determining the relationship and tradeoff between the average energy. $\xi_{av} = \sum_{i=1}^{M} p_A(x_i)\, E(x_i)$ and entropy $H(x) = \sum_{i=1}^{M} p_A(x_i) \log_2(p_A(x_i))$, the coefficient $A(\lambda)$ must be chosen to make $\sum p_A(x) = 1$ [26].

The entropy value determines the optimal pmf through the λ value. As λ approaches 0, the distribution becomes uniform more, while it becomes more like a reduced variance Gaussian distribution as λ increases.

The Water Circle Algorithm (WCA) will be used to estimate parameters for a Maxwell-Boltzmann distribution model fitted to MMRDM probabilities from PAS 64-QAM symbols generated with L = 100. The estimated parameters of MB distribution are $\lambda = 0.0454$ and $A(\lambda) = 0.2399$.

The Gaussian distribution can be approached by the Maxwell-Boltzmann distribution, which is governed by the value of the rate parameter $\boldsymbol{\lambda}$ and the order of modulation M. The formula for the Gaussian distribution is as follows:

$$f(x) = a.e^{\left(\frac{-(x-\mu)^2}{2\sigma^2}\right)} \quad (10)$$

The amplitude is a, the mean value is μ, and the Gaussian curve standard deviation is σ. By comparing Equations 9 and 10, the Gaussian fit, f(x) parameter a = 0.2399, μ = 0 due to symmetric, and σ^2= 11.016, where a = A(λ) , and σ^2=1⁄2λ and as shown in Figure 3.

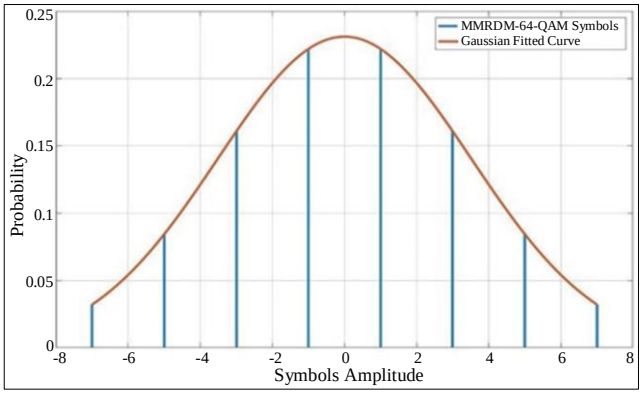

Fig. 3 Probability distribution of one dimension of MMRDM-64-QAM with its Gaussian fit

4. Proposed Probabilistic Shaping Performance

4.1. Performance over AWGN Channel

The best detection scheme for a probabilistic shaping modulator is the Maximum A Posteriori (MAP) detector. This detector considers the prior symbol distribution, while the Maximum Likelihood Detector (MLD) does not [7, 8]. The Symbol Error Rate (SER) can be defined by the following expression [8]:

$$P_{s|M-QAM} = \alpha Q\left(\sqrt{\epsilon \frac{E_s}{N_0}}\right) - \alpha Q^2\left(\sqrt{\epsilon \frac{E_s}{N_0}}\right) \quad (11)$$

α is the nearest neighbor's average number in the symbol constellation, and $\epsilon = {}^{2}/_{\xi_{av}}$. For square M-QAM, there are $(M - 4\sqrt{M} + 4)$ points with four neighbors, three neighbors for the $(4\sqrt{M} - 8)$ edge points and two neighbors for four corner points. α can be calculated as:

$$\alpha = \frac{\frac{1}{c1}+\frac{1}{c2}+\ldots+\frac{1}{cL}}{L} \times 4 + \frac{\frac{1}{c1}+\frac{1}{c2}+\ldots+\frac{1}{cL}}{L} \times 4 + \cdots + \frac{\frac{1}{cL}}{L} \times 2 \quad (12)$$

And average symbols energy is,

$$\xi_{av} = \frac{\frac{1}{c1}+\frac{1}{c2}+\ldots+\frac{1}{cL}}{L} E(x_1) + \frac{\frac{1}{c1}+\frac{1}{c2}+\ldots+\frac{1}{cL}}{L} E(x_2) + \cdots + \frac{\frac{1}{cL}}{L} E(x_M) \quad (13)$$

Substitute Equations 12 and 13 in Equation 11 to calculate the symbol error rate at certain SNRs. Let's take the 16-QAM as an example; for uniform distribution QAM, the calculated α and ξ_{av} are 3 and 10; from Equation 11, the value of SNR is 19 dB, which gives SER = 10^{-4}.

For PAS-QAM with H=3.55 bits/symbol and $\lambda = 0.0341$, the symbols probabilities $p_A(a^{16})$ are shown in Equation 6, and the estimated values of α and ξ_{av} from Equations 12 and 13 are 3.5 and 6, according to Equation 11, SER =10^{-4} at SNR =16.86 dB.

The improvement gained in SNR is about 2.2 dB. The formula in Equation 11 is simple to calculate and is considered a good approximation of the symbol error ratio across the AWGN channel.

4.2. Performance over Fading Channels

In a wireless communication channel where fading occurs, the power of the received signal is affected by a random variable known as the channel coefficient, h. The instantaneous SNR per symbol, γ, is calculated as $\gamma = |h|^2 \, Es/No$, while the average SNR is $\bar{\gamma} = \overline{|h|}^2 Es/No$.

To evaluate the average symbol error probability, the integral of the AWGN symbol error probability $P_{s|M-QAm}(\gamma)$ over fading Probability Density Function (PDF) $p_\gamma(\gamma)$ must be estimated using the following formula [6]:

$$P_{s|Fading} = \int_0^\infty P_{s|M-QAM}(\gamma) p_\gamma(\gamma) d\gamma \quad (14)$$

A noncomplicated formula of the Symbol Error Ratio (SER) in fading channel models is presented, which includes Rayleigh, Log-normal, Nakagami-m, and Composite Log-Normal shadowing/Nakagami-m fading channels with possible conditions.

4.2.1. Performance over Rayleigh Channel

The Rayleigh channel is the perfect choice for analyzing fading channels. It offers the simplest yet most effective way to study the instantaneous SNR per bit PDF, with PDF formulated as:

$$p_\gamma(\gamma) = \frac{1}{\bar{\gamma}} \exp\left(-\frac{\gamma}{\bar{\gamma}}\right), \ \gamma \geq 0 \quad (15)$$

Substituting Equations 11 and 15 in Equation 14, we estimate the probability of a symbol error of PAS-MMRDM in the Rayleigh channel using the following formula [6, ch.5, 9].

$$P_{s|Rayleigh} = \alpha\left(1 - \sqrt{\frac{\epsilon\bar{\gamma}}{1+\epsilon\bar{\gamma}}}\right) - \frac{\alpha}{2}\left(1 - \sqrt{\frac{\epsilon\bar{\gamma}}{1+\epsilon\bar{\gamma}}} * \frac{4}{\pi}\tan^{-1}\left(\sqrt{\frac{1+\epsilon\bar{\gamma}}{\epsilon\bar{\gamma}}}\right)\right) \quad (16)$$

For the same conditions applied in section 4 and for the same values of α, ϵ, and SER, the power of channel coefficient is $|h|^2 = 1$, the improvement gained in SNR is about 1.579 dB. Again, there is no need for complex calculations to obtain SER for the Rayleigh channel.

4.2.2. Performance over Log-Normal Channel

The performance of terrestrial and satellite land-mobile communication systems is affected by shadowing from different obstacles, either natural or human-made. For various environments, indoor or outdoor, the Log-normal distribution

is the mathematical model utilized to express the Log-normal fading $p_\gamma(\gamma)$ as [9, 10, 27]:

$$p_\gamma(\gamma) = \frac{1}{\sqrt{2\pi\sigma_\gamma^2\,\gamma}} \exp\left(-\frac{(\ln(\gamma)+\mu)^2}{2\sigma_\gamma^2}\right) \gamma \geq 0 \qquad (17)$$

Where, σ_γ^2 and $\mu = \sigma_\gamma^2/2$ are the variance and mean of Log-normal fading with random variable $\ln(\gamma)$. When substituting Equations 11 and 17 in Equation 14, Gauss-Hermite integration can be used to evaluate the resultant integration to estimate the probability of symbol error of PAS-MMRDM in Log-normal fading as in the following formula [6, Ch.5, 9, 10].

$$P_{s|Lognormal} = \frac{\alpha}{\sqrt{\pi}} \sum_{i=1}^{N_p} w_{xi}\, Q\left(\mathrm{e}^{(x_i\sqrt{2\sigma_\gamma^2}+\mu)}\sqrt{\epsilon\gamma}\right) - \frac{\alpha}{2\sqrt{\pi}} \sum_{i=1}^{N_p} w_{xi}\, Q^2\left(\mathrm{e}^{(x_i\sqrt{2\sigma_\gamma^2}+\mu)}\sqrt{\epsilon\gamma}\right) \qquad (18)$$

x_i and w_{xi} represent the zeros and weight factors of *Np*-order Hermite polynomial, and i=1,2,…, Np, respectively and are given by [28, Table (25.10)]. The order of polynomial Np affects the accuracy of the symbol error probability.

From Equation 18, the gain in SNR in the Log-normal channel is 1.95 (dB) for the same assumptions used in previous subsections and for the same values of α, ϵ, and SER, with variance of fading $\sigma_\gamma^2 = 0.2$, and polynomial order, Np = 20.

4.2.3. Performance over Nakagami-m Channel

Practically, the communication link between two nodes may experience different fading conditions. Here, the Nakagami-m distribution is a suitable distribution with an m parameter that can be used to model a mathematically wide range of fading scenarios, including special cases like m = 0.5, a Gaussian distribution with one side.

When m =1, this will represent Rayleigh fading and other distributions. The Nakagami-m PDF can given by [6, 11].

$$p_\gamma(\gamma) = \frac{1}{\Gamma(m)}\left(\frac{m}{\bar{\gamma}}\right)^m \exp\left(-\frac{m\gamma}{\bar{\gamma}}\right), \ \gamma \geq 0 \qquad (19)$$

Where m, $\Gamma(\cdot)$ is the fading parameter and gamma function, respectively.

The symbol error performance can evaluated by solving the integration resulting from substitute Equations 11 and 19 in Equation 14. Using the derived definite integral in [6, Appendix 5A:5], this closed-form expression can be evaluated as [11].

$$P_{s|Nakagami-m} = \begin{cases} \frac{\alpha}{2}(1-\beta I_o) - \frac{\alpha}{4}\left(1 - \frac{4}{\pi}\beta\left\{\begin{matrix}\left(\frac{\pi}{2} - tan^{-1}\beta\right) I_o \\ + sin^{-1}(tan^{-1}\beta)\,\Theta_o\end{matrix}\right\}\right), \\ m = integer \\ \alpha \frac{1}{2\sqrt{\pi}} \frac{\sqrt{c}}{(1+c)^{m+0.5}} \frac{\Gamma\left(m+\frac{1}{2}\right)}{\Gamma(m+1)} \times F_1\left(1; m+\frac{1}{2}; m+1; \frac{1}{1+c}\right), \\ m = noninteger \end{cases} \qquad (20)$$

Where,

$\beta = \sqrt{\frac{c}{1+c}}$,

$c = \frac{\epsilon\gamma}{2m}$,

$I_o = \sum_{k=0}^{m-1} \binom{2k}{k} \left(\frac{1-\beta^2}{4}\right)^k$,

$\Theta_o = \sum_{k=1}^{m-1} \sum_{i=1}^{k} \frac{T_{ik}}{\left(1+\frac{\epsilon\gamma}{m}\right)^k} [\cos(\tan^{-1}\beta)]^{2(2k-i)+1}$,

$T_{ik} = \frac{\binom{2k}{k}}{\binom{2(k-i)}{k-i} 4^i [2(k-i)+1]}$, and

$F_1(.;.;.;.)$ is hypergeometric function.

The value of m spans the Nakagami-m distribution over many fading scenarios; as an example applied before, let's set the value of m to 1, and Nakagami-m becomes Rayleigh fading. The parameters α, ϵ, and SER applied in previous subsections will be the same, and the SNR gain will be approximately the same as gained in subsection 4.2.1, which is 1.579 (dB).

4.2.4. Performance over Composite Channel (Log-Normal Shadowing/Nakagami-m)

The Composite fading channel (Log-normal Shadowing / Nakagami-m) is used to model the congested areas downtown, which contain a large number of objects at a slow speed, like pedestrians and vehicles. To obtain pγ (γ), the instantaneous fading of Nakagami-m in Equation 19 is averaging over conditional Log-normal fading PDF in Equation 17; the resultant is composite PDF as [2, 12].

$$p_\gamma(\gamma) = \int_0^\infty \frac{1}{\Gamma(m)}\left(\frac{m}{\Psi}\right)^m exp\left(-\frac{m\gamma}{\Psi}\right) \times \left\{\frac{1}{\sqrt{2\pi\sigma_\Psi^2\,\Omega}} \exp\left(-\frac{(\ln(\Psi)+\mu)^2}{2\sigma_\Psi^2}\right)\right\} d\Psi \qquad (21)$$

As mentioned before, Gauss–Hermite quadrature integration with order Np will be used to compute the inner integral, and the closed integral form will be used to obtain the following symbol error probability formula [12]:

$$P_{s|Composite} = \begin{cases} \frac{\alpha}{2\sqrt{\pi}}\sum_{j=1}^{Np} w_{xj}(1-\beta I_o) - \\ \frac{\alpha}{4\pi}\sum_{j=1}^{Np} w_{xj}\left(1-\frac{4}{\pi}\beta\left\{\begin{matrix}\left(\frac{\pi}{2}-tan^{-1}\beta\right)I_o \\ +\,sin^{-1}(tan^{-1}\beta)\,\theta_o\end{matrix}\right\}\right), \\ m = integer \\ \alpha\frac{1}{2\sqrt{\pi}}\sum_{j=}^{Np} w_{xj}\left\{\begin{matrix}\frac{\sqrt{c}}{(1+c)^{m+0.5}}\frac{\Gamma\left(m+\frac{1}{2}\right)}{\Gamma(m+1)}\times \\ F_1\left(1;m+\frac{1}{2};m+1;\frac{1}{1+c}\right)\end{matrix}\right\}, \\ m = noninteger \end{cases} \quad (22)$$

All parameters of Equation 22 are the same parameters defined in previous subsections except $\beta = \sqrt{\frac{c_j}{1+c_j}}$, and $c_j = \frac{\epsilon\gamma}{2m} e^{(x_j\sqrt{2\sigma_\gamma^2}+\mu)}$. For m = 1, $\sigma_\gamma^2 = 0.2$, and the order of polynomial Np = 20, the SNR improvement is about 1.722 dB at higher values of SNR than Rayleigh or Nakagami-m fading channels for the same value of the parameters α, ϵ used in AWGN channel, where α and ϵ values are 3, 10 for uniform 16-QAM respectively and 3.5, 6 for PAS-MMRDM with L = 3 and subgroups are c1 =4, c2 = 8, and c3 = 16.

5. Discussion and Results

5.1. AWGN Channel

The theoretical SER of PAS-MMRDM given by Equation 11 supported by MATLAB simulation is shown in Figure 4, where the M-QAM SER with uniform distribution is also included for comparison. As illustrated in the figure, the improvement in the performance of the PAS-16-QAM system is about 4 dB and 2.1dB in SNR when H={3.1,3.6}bits/symbol where the rate factor (λ) values = (0.1733 and 0.0683) and L={10,30}.

At the same time, for PS-64-QAM, the H= {4.6,5.5} bits/symbol is used for the λ (0.1062,0.06868) and levels (80,100) will be the improvement in SNR about 4.86 and 2.88 dB respectively, and finally the values of the λ (0.0587,0.02947) for H={6.4,7.4} bits/symbol when L (300,360) was used on the PAS-256-QAM system, the improvement in SNR will be 5.1 and 3.36 dB respectively.

All results are compared to the QAM system with a uniform distribution at SER = 10^{-4}. It is also noted from the results that the improvement in the SNR depends on the rate factor λ, which in turn depends entirely on the number of levels (L) and repetition groups (ci) for each level according to the modulation order-M.

Another comparison of SER performance will be made between PS-M-QAM and a regular QAM of lower order M/4 with the same entropy values, which are 4, 6, and 8 bits/symbol, as shown in Figure 5. PS-M-QAM improves SER compared to regular QAM whenever the modulation rank M has increased, as the SNR gain is about 1.21 dB when comparing PAS-64-QAM with regular 16-QAM at 4 bit/symbol entropy. The obtained SNR gain is 1.64 dB when comparing PS-256-QAM with uniform 64-QAM and 6-bit/symbol entropy. Finally, the SNR gain will be about 1.81 dB at H=8 bits/symbol and PAS-1024-QAM against regular 256-QAM. All cases of SNR gain are measured at SER = 10^{-4}.

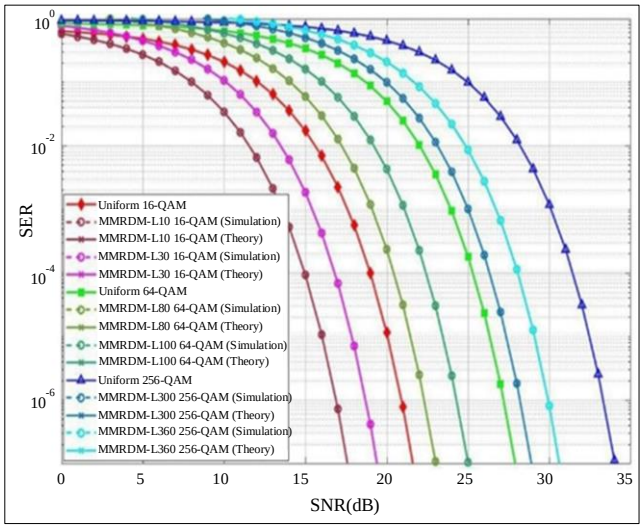

Fig. 4 Uniform M-QAM and PAS_MMRDM error performance under AWGN channel condition

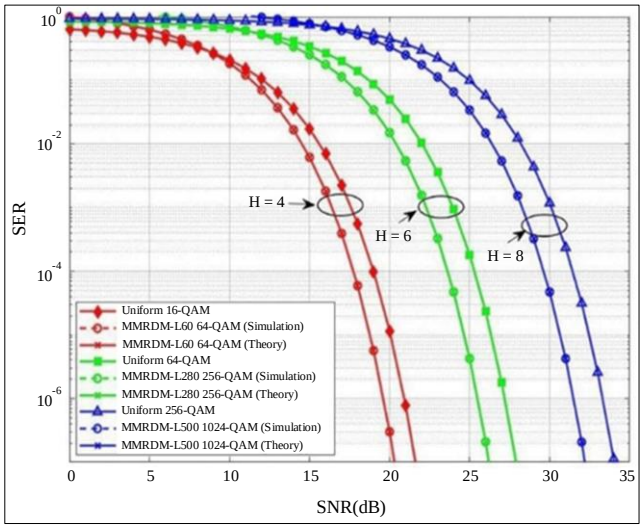

Fig. 5 Uniform M-QAM and PAS_MMRDM error performance at the same entropies H

5.2. Fading Channels

Under the condition of Rayleigh fading, the MATLAB simulation results of SER and the theoretical PAS-MMRDM SER were evaluated using Equation 16 with SER of uniform M-QAM, which are illustrated in Figure 6. Similar to the previous cases in the AWGN subsection, modulation order M is 16, 64, and 256; the entropies, number of levels L, and repeated subgroups ci are the same.

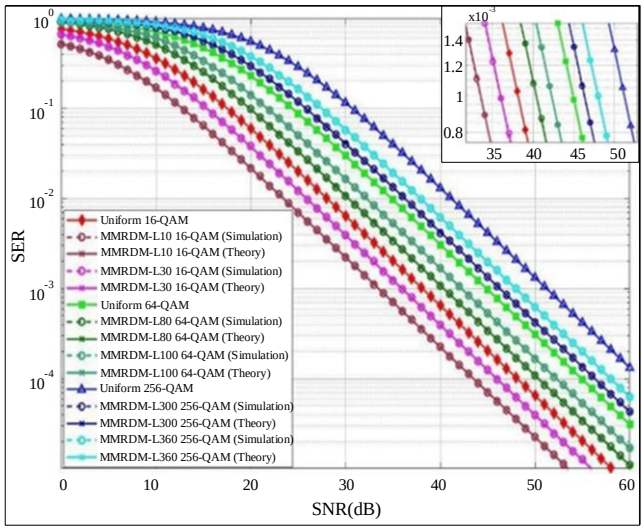

Fig. 6 Symbol Error Rate of uniform M-QAM and PAS in rayleigh fading channel

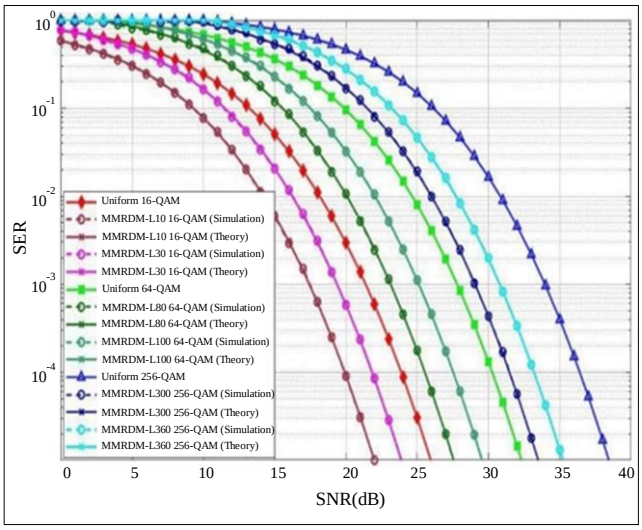

Fig. 8 Symbol Error Rate of PAS and uniform M-QAM in log-normal fading channel

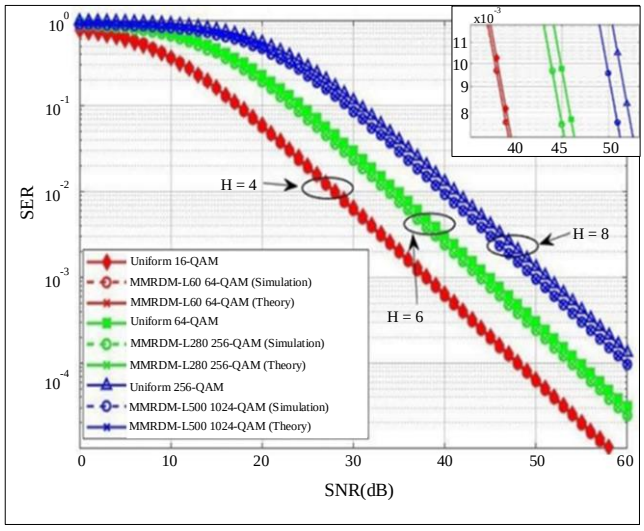

Fig. 7 Symbol Error Rate of uniform M-QAM and PAS in rayleigh fading channel at equal entropies H

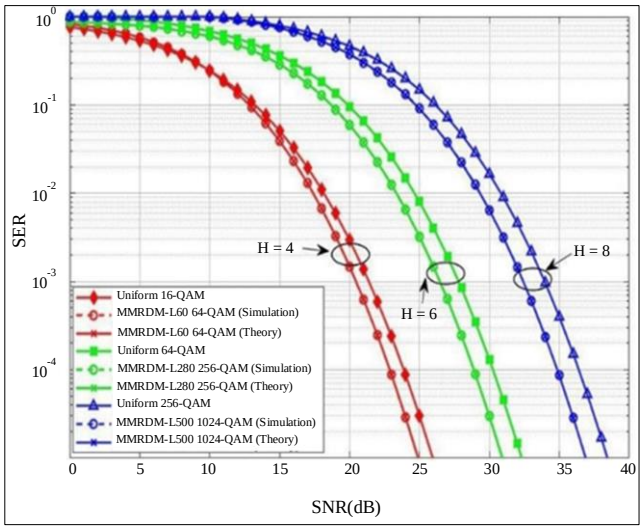

Fig. 9 Symbol Error Rate of PAS and uniform M-QAM in log-normal fading channel at equal entropies H

The SNR improvement for PAS-MMRDM over uniform distribution is 4.6,2.1 dB for PAS-16QAM, 4.6,2.65 dB for PAS-64QAM, and 4.9, 3.3 dB for PAS-256 QAM. While for cases where the entropies (4, 6, and 8) bits/symbol, the evaluated gains in SNR are 0.29 dB, 1.07 dB, and 1.38 dB, as shown in Figure 7, all Rayleigh fading cases evaluated at SER = 10^{-3}. Figure 7 shows that PAS-MMRDM improves the system performance regarding SER compared with the uniform M-QAM, which is higher in order even in Rayleigh fading.

The theoretical (estimated from Equation 18) and simulation results of SER performance of compared PAS-QAM with uniform QAM, under Log-normal fading with fading variance σ_γ^2 = 0.1, are shown in Figures 8 and 9. All parameters of MMRDM in 4.1 will be used here.

In all cases, PAS-MMRDM improved SNR for all modulation order M, even when compared at the same entropy, as shown in Figure 9. For instance, in Figure 8 and at SER = 10^{-4}, the SNR gains are about 4 and 2.1 dB for PAS-16-QAM, 4.6 and 2.88 dB for PAS-64-QAM and finally 5 and 3.37 dB for PAS-256-QAM. The role is to repeatedly compare SER performance at equal entropy using entropy (H) of 4 bits/symbol to compare PAS-64QAM with regular 16-QAM, compare PAS-256QAM with regular 64QAM at the entropy of 6 bits/symbol, and finally compare PAS-1024QAM with uniform 256QAM at a net entropy of 8 bits/symbol, as was used in the AWGN channel in the previous subsection.

Figure 9 shows the comparison results. From Figure 9, an SNR gain of about 1 dB was obtained at 4-bit entropy, 1.35 dB at H=6-bit, and finally, the gain was about 1.52 dB at H =

8-bit. All cases were measured at SER=10^{-4}, as previously mentioned. It is concluded from the previous results that PAS-MMRDM gives superior performance over the log-normal fading channel but less than it does over the AWGN channel. For the Nakagami-m fading channel, the error performance will be evaluated for two special cases: first, m = 0.5 (one side Gaussian), and the other case, m =1 (Rayleigh distribution). Again, the same parameters of MMRDM mentioned before will be used here.

Figure 10 shows the comparison in error performance between the proposed method (theoretical and simulation) and uniform M-QAM in case m=0.5; the inset shows the enhancement in SNR at particular SER = 10^{-2}. The SNR gained are {3.9,1.44} for PAS-16QAM at H={3.1,3.6}, for PAS-64QAM SNR gains are {4,2.12} at entropies {4.6,5.5}, and SNR gains {4.5,3} for PAS-256QAM at entropies H={6.4,7.4}.

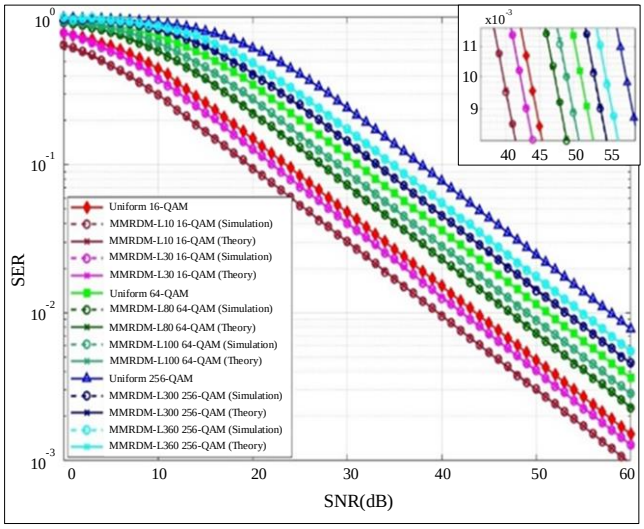

Fig. 10 M-QAM symbol error rate in nakagami-m channel at m = 0.5

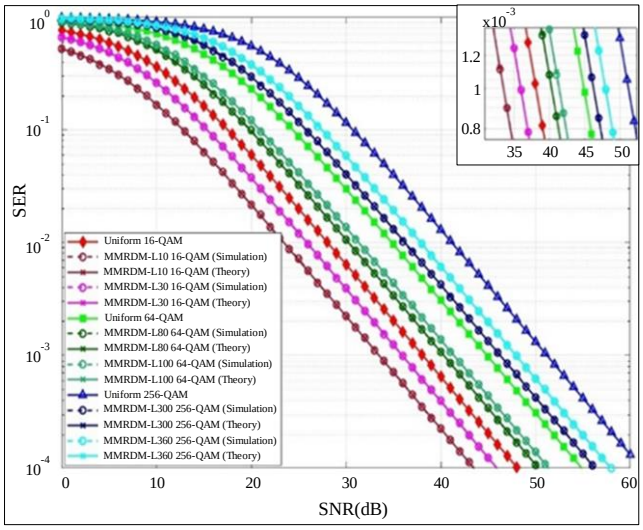

Fig. 11 M-QAM symbol error rate in nakagami-m channel at m = 1

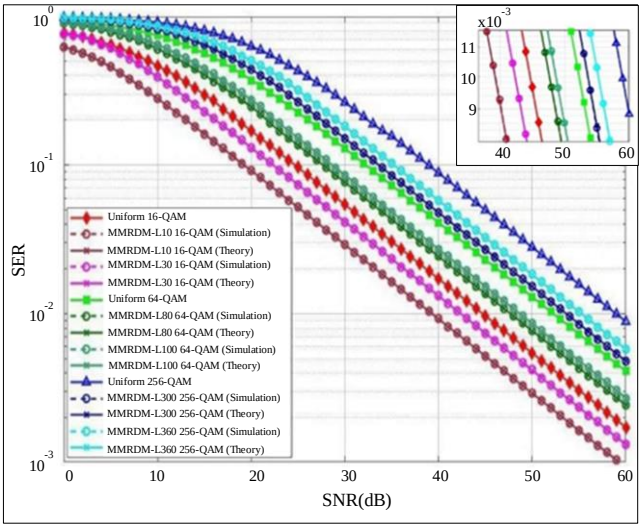

Fig. 12 M-QAM symbol error rate in composite channel (log-normal shadowing/nakagami-m) at m=0.5

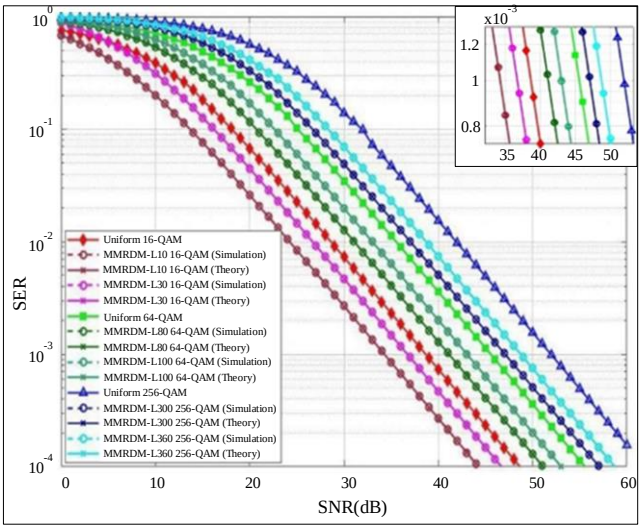

Fig. 13 M-QAM symbol error rate in composite fading channel (log-normal shadowing/nakagami-m) at m=1

Meanwhile, Figure 11 illustrates the compared symbol error performance at m =1. As shown in Figure 11, the error performance for Nakagami-m at m = 1 is similar to that in the Rayleigh channel, as shown in Figure 6. The summary of results is the SNR gains {4.7, 2.2} for PAS-16QAM, SNR gains {4.9, 3.45} for PAS-64QAM, and finally, the SNR gains {5, 3.6} for PAS-256QAM, all results at the same entropies used earlier. The proposed scheme introduces a reasonable SNR gain or SER enhancement even in the worst Nakagami-m conditions.

Figures 12 and 13 show the results of the Composite fading channel (Log-Normal shadowing/Nakagami-m). Figure 12 shows the results of error performance for case m =0.5 and Log-normal fading variance σ_γ^2=0.1. Another case will be examined at m =1, as shown in Figure 13.

In all cases, the proposed method offers a good improvement in Symbol Error Ratio (SER) at specific SNR compared to uniformly distributed M-QAM. For instance, for m=0.5 and at SER = 10^{-2} the SNR enhancement about {4,1.38} dB for PAS-16QAM, {4.2, 2.01} dB for PAS-64QAM, and {4.9, 2.9} dB for PAS-256QAM.

Meanwhile, Figure 13 illustrates the compared symbol error performance at m =1 for the composite fading channel. For the same entropies used before, the summary of results is the SNR gains {4.5, 2.01} for PAS-16QAM, SNR gains {4.8, 3.15} for PAS-64QAM, and finally, the SNR gains {4.9, 3.45} for PAS-256QAM. Again, the proposed scheme introduces an excellent SNR gain and SER enhancement in composite fading channel conditions.

6. Conclusion

The proposed method's Symbol Error Ratio (SER) was estimated using mathematical relationships, supported by MATLAB simulation, and compared to a uniformly distributed square QAM across the mentioned channels. This work presented a framework on how the proposed method introduces a trading-off between spectral efficiency and energy efficiency and the effect of parameters, the most important of which is the number of levels L on the signal distribution, which affects the entropy and thus affects the performance of the method.

The Water Cycle Algorithm (WCA) was used to choose the optimal parameters so that the distribution of the generated symbols matches the optimal distribution. The ease and flexibility of this method in generating symbols that follow the required distribution by changing the parameter levels (L) or changing the repetition groups at each level were also demonstrated.

According to the results of the study, probabilistic modulation techniques are considered an excellent choice for application in communications systems, especially fifth and sixth-generation technologies. However, this technology is used in optical communications and ATSC broadcasts. According to the results, the system's immunity to noise and fading improved, and it became more efficient and reliable in data transmission thanks to PAS, which improved the SNR gain. PAS technologies are essential for applications in which power consumption plays a key role because, using PAS, it is possible to design highly energy-efficient communications systems with good spectral efficiency.

Further study might focus on examining the Bit Error Ratio (BER) performance of the PAS-MMRDM. The BER analysis of the suggested distribution matcher will depend on the selected Forward Error Correction (FEC) method. Integrating the process of shaping with coding at optimum rates would further improve the SNR gain.

Another study can be conducted on the use of optimization to choose the optimal distribution in terms of probabilistic shaping to enhance the system's performance with regard to SER or improve the Achieved Informational Rate (AIR) in any communications channel. For example, AIR is calculated and sent to the optimizer to generate symbols with an ideal distribution that achieves the required rate. In the proposed method, the optimal distribution is obtained by changing the number of levels L and repeating subgroups, just as WCA was used to improve the SNR gain.

References

[1] Latif U. Khan et al., "Digital-Twin-Enabled 6G: Vision, Architectural Trends, and Future Directions," *IEEE Communications Magazine*, vol. 60, no. 1, pp. 74-80, 2022. [CrossRef] [Google Scholar] [Publisher Link]

[2] Li You et al., "Energy Efficiency and Spectral Efficiency Tradeoff in RIS-Aided Multiuser MIMO Uplink Transmission," *IEEE Transactions on Signal Processing*, vol. 69, pp. 1407-1421, 2020. [CrossRef] [Google Scholar] [Publisher Link]

[3] Shanzhi Chen et al., "Vision, Requirements, and Technology Trend of 6G: How to Tackle the Challenges of System Coverage, Capacity, User Data-Rate and Movement Speed," *IEEE Wireless Communications*, vol. 27, no. 2, pp. 218-228, 2020. [CrossRef] [Google Scholar] [Publisher Link]

[4] Fred Buchali et al., "Rate Adaptation and Reach Increase by Probabilistically Shaped 64-QAM: An Experimental Demonstration," *Journal of Lightwave Technology*, vol. 34, no. 7, pp. 1599-1609, 2016. [CrossRef] [Google Scholar] [Publisher Link]

[5] F.R. Kschischang, and S. Pasupathy, "Optimal Nonuniform Signaling for Gaussian Channels," *IEEE Transactions on Information Theory*, vol. 39, no. 3, pp. 913-929, 1993. [CrossRef] [Google Scholar] [Publisher Link]

[6] Marvin K. Simon, and Mohamed-Slim Alouini, *Digital Communication over Fading Channels*, Wiley, 2004. [CrossRef] [Google Scholar] [Publisher Link]

[7] John G. Proakis, *Digital Communications*, McGraw-Hill, Higher Education, 3rd ed., 1995. [Google Scholar] [Publisher Link]

[8] Kyongkuk Cho, and Dongweon Yoon, "On the General BER Expression of One-and Two-Dimensional Amplitude Modulations," *IEEE Transactions on Communications*, vol. 50, no. 7, pp. 1074-1080, 2002. [CrossRef] [Google Scholar] [Publisher Link]

[9] Tilahun Zerihun Gutema, Harald Haas, and Wasiu O. Popoola, "On Symbol Error Performance of Probabilistic Shaping in Noise-Limited and Fading Channels," *IEEE Open Journal of the Communications Society*, vol. 4, pp. 1218-1228, 2023. [CrossRef] [Google Scholar] [Publisher Link]

[10] Ha Duyen Trung, "Performance Analysis of FSO DF Relays with Log-Normal Fading Channel," *Journal of Optical Communications*, vol. 44, no. 3, pp. 395-403, 2023. [CrossRef] [Google Scholar] [Publisher Link]

[11] Hugerles S. Silva et al., "Closed-Form Expression for the Bit Error Probability of the M-QAM for a Channel Subjected to Impulsive Noise and Nakagami Fading," *Wireless Communications and Mobile Computing*, vol. 2018, pp. 1-9, 2018. [CrossRef] [Google Scholar] [Publisher Link]

[12] Juan Reig et al., "Log-Moment Estimators of the Nakagami-Lognormal Distribution," *EURASIP Journal on Wireless Communications and Networking*, vol. 2019, no. 1, pp. 1-10, 2019. [CrossRef] [Google Scholar] [Publisher Link]

[13] G.D. Forney, and L.F. Wei, "Multidimensional Constellations. I. Introduction, Figures of Merit, and Generalized Cross Constellations," *IEEE Journal on Selected Areas in Communications*, vol. 7, no. 6, pp. 877-892, 1989. [CrossRef] [Google Scholar] [Publisher Link]

[14] Yunus Can Gültekin et al., "Enumerative Sphere Shaping for Wireless Communications with Short Packets," *IEEE Transactions on Wireless Communications*, vol. 19, no. 2, pp. 1098-1112, 2020. [CrossRef] [Google Scholar] [Publisher Link]

[15] Stella Civelli, and Marco Secondini, "Hierarchical Distribution Matching for Probabilistic Amplitude Shaping," *Entropy*, vol. 22, no. 9, pp. 1-27, 2020. [CrossRef] [Google Scholar] [Publisher Link]

[16] Fernando P. Guiomar et al., "Adaptive Probabilistic Shaped Modulation for High-Capacity Free-Space Optical Links," *Journal of Lightwave Technology*, vol. 38, no. 23, pp. 6529-6541, 2020. [CrossRef] [Google Scholar] [Publisher Link]

[17] Evgeny Bobrov, and Adyan Dordzhiev, "On Probabilistic QAM Shaping for 5G MIMO Wireless Channel with Realistic LDPC Codes," *arXiv*, pp. 1-15, 2023. [CrossRef] [Google Scholar] [Publisher Link]

[18] Georg Böcherer, Fabian Steiner, and Patrick Schulte, "Bandwidth Efficient and Rate-Matched Low-Density Parity-Check Coded Modulation," *IEEE Transactions on Communications*, vol. 63, no. 12, pp. 4651-4665, 2015. [CrossRef] [Google Scholar] [Publisher Link]

[19] Patrick Schulte, and Georg Böcherer, "Constant Composition Distribution Matching," *IEEE Transactions on Information Theory*, vol. 62, no. 1, pp. 430-434, 2016. [CrossRef] [Google Scholar] [Publisher Link]

[20] Patrick Schulte, and Fabian Steiner, "Divergence-Optimal Fixed-to-Fixed Length Distribution Matching with Shell Mapping," *IEEE Wireless Communications Letters*, vol. 8, no. 2, pp. 620-623, 2019. [CrossRef] [Google Scholar] [Publisher Link]

[21] Shiwei Wang et al., "26.8-m THz Wireless Transmission of Probabilistic Shaping 16-QAM-OFDM Signals," *APL Photonics*, vol. 5, no. 5, 2020. [CrossRef] [Google Scholar] [Publisher Link]

[22] Yao Yao, "Design and Analysis of Rotated-QAM Based Probabilistic Shaping Scheme for Rayleigh Fading Channels," *IEEE Transactions on Wireless Communications*, vol. 19, no. 5, pp. 3047-3063, 2020. [CrossRef] [Google Scholar] [Publisher Link]

[23] Tilahun Z. Gutema, and Wasiu O. Popoola, "Single LED Gbps Visible Light Communication with Probabilistic Shaping," *2021 IEEE Global Communications Conference (GLOBECOM)*, Madrid, Spain, pp. 1-6, 2021. [CrossRef] [Google Scholar] [Publisher Link]

[24] Sidrah Javed et al., "When Probabilistic Shaping Realizes Improper Signaling for Hardware Distortion Mitigation," *IEEE Transactions on Communications*, vol. 69, no. 8, pp. 5028-5042, 2021. [CrossRef] [Google Scholar] [Publisher Link]

[25] Tilahun Zerihun Gutema, Harald Haas, and Wasiu O. Popoola, "WDM Based 10.8 Gbps Visible Light Communication with Probabilistic Shaping," *Journal of Lightwave Technology*, vol. 40, no. 15, pp. 5062-5069, 2022. [CrossRef] [Google Scholar] [Publisher Link]

[26] Ali Shaban Hassooni, and Laith Ali Abdul Rahaim, "FPGA Based Modified Multi-Repeat Distribution Matcher for Probabilistic Amplitude Shaping," *Nexo Scientific Magazine*, vol. 36, no. 5, pp. 108-121, 2023. [CrossRef] [Google Scholar] [Publisher Link]

[27] Majid Safari, and Murat Uysal, "Relay-Assisted Free-Space Optical Communication," *IEEE Transactions on Wireless Communications*, vol. 7, no. 12, pp. 5441-5449, 2008. [CrossRef] [Google Scholar] [Publisher Link]

[28] Milton Abramowitz, Irene A. Stegun, *Handbook of Mathematical Functions with Formulas, Graphs, and Mathematical Tables*, Washington US Govt Print, 2006. [Google Scholar] [Publisher Link]

[29] Zexuan Jing et al., "A Multi-Repeat Mapping Based Probabilistic Shaping Coding Method Applied to Data Center Optical Networks," *Optical Fiber Technology*, vol. 61, pp. 1-7, 2021. [CrossRef] [Google Scholar] [Publisher Link]